

SNUST-01-0902
 KIAS-P01045
 PUPT-2008
 hep-th/0110215

Interacting Open Wilson Lines from Noncommutative Field Theories ¹

Youngjai Kiem ^{a,d}, Sangmin Lee ^b, Soo-Jong Rey ^c, Haru-Tada Sato ^a

BK21 Physics Research Division & Institute of Basic Science

Sungkyunkwan University, Suwon 440-746 KOREA ^a

School of Physics, Korea Institute for Advanced Study, Seoul 130-012 KOREA ^b

School of Physics & Center for Theoretical Physics

Seoul National University, Seoul 151-747 KOREA ^c

Physics Department, Princeton University, Princeton, NJ 08544 USA ^d

ykiem, haru@newton.skku.ac.kr, sangmin@kias.re.kr, sjrey@gravity.snu.ac.kr

abstract

In noncommutative field theories, it was known that one-loop effective action describes propagation of non-interacting open Wilson lines, obeying the flying dipole's relation. We show that two-loop effective action describes cubic interaction among 'closed string' states created by open Wilson line operators. Taking d-dimensional $\lambda[\Phi^3]_\star$ -theory as the simplest setup, we compute nonplanar contribution at low-energy and large noncommutativity limit. We find that the contribution is expressible in a remarkably simple cubic interaction involving scalar open Wilson lines only and nothing else. We show that the interaction is purely geometrical and noncommutative in nature, depending only on sizes of each open Wilson line.

¹ Work supported in part by the BK-21 Initiative in Physics, the KRF International Collaboration Grant, the KRF Grant 2001-015-DP0082, the KOSEF Interdisciplinary Research Grant 98-07-02-07-01-5, the KOSEF Leading Scientist Program, and the KOSEF Brain-Pool Program.

1 Introduction

The most significant feature of generic noncommutative field theories is phenomenon of the UV-IR mixing [1]. Recently, it is asserted that open Wilson lines (OWLs) [2, 3, 4] are responsible for the phenomenon [5]: long-distance excitations described by the open Wilson lines correspond to noncommutative dipoles [6, 7] (direct analogs of the Mott excitons [5] in metal under a strong magnetic field), and accounts for the peculiar long-distance dynamics in noncommutative field theories. It also implies that the open Wilson lines ought to be ubiquitous to any noncommutative field theory, be it gauge invariant or not, or Poincaré invariant or not. A partial evidence for the ubiquity is provided by the spin-independence of the generalized \star_N -product [8]. Based on the insight, in [9, 10], it was proven that the nonplanar part of the complete one-loop effective action of a noncommutative *scalar* field theory is expressible entirely in terms of open Wilson lines — and nothing else — in a remarkably simple form. This feature is in support of the conjecture [5] that, as in $s - t$ channel duality in open and closed string theories [11], quantum dynamics of elementary field is described, at long distance, by classical dynamics of open Wilson line. This duality underlies the phenomenon of UV-IR mixing, and is quantified by the following relation between dipole moment and energy-momentum four-vectors:

$$\ell^m = \theta^{mn} k_n, \quad (1.1)$$

nicknamed as ‘flying dipole’s relation’ [5].

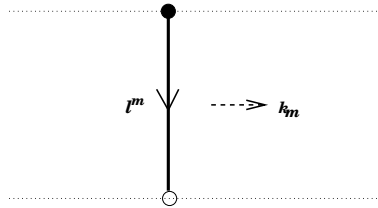


Figure 1: *Spacetime view of open Wilson line propagation. The noncommutativity is turned on the plane spanned by the two vectors, ℓ^m and k_m .*

The result of [9][10] indicates that the one-loop effective action describes propagation of a non-interacting open Wilson line and takes schematically the form:

$$\Gamma_2[W(\Phi)] = \frac{1}{2} \text{Tr}_{\mathcal{H}_{\text{dipole}}} \left(\widehat{W} \cdot \mathcal{K}_{-\frac{d}{2}} \cdot \widehat{W} \right), \quad (1.2)$$

where the scalar Wilson line operator is defined as

$$W_k[\Phi] = \int d^d x \mathcal{P}_\tau \exp_\star \left(-g \int_0^1 d\tau |\dot{y}(\tau)| \Phi(x + y(\tau)) \right) \star e^{ik \cdot x}, \quad (1.3)$$

$\mathcal{H}_{\text{dipole}}$ refers to a one-‘dipole’ Hilbert space, and $\mathcal{K}_{-\frac{d}{2}}$ denotes spacetime propagation kernel of the dipole.

In this paper, we shall be extending earlier analysis to two-loop level, and study interaction among ‘closed string’ states created by the open Wilson line operators. The main results are (1) the two-loop effective action is expressible in terms of interaction among the noncommutative dipoles created by the open Wilson lines, (2) interaction is cubic, and is entirely geometrical, as dictated by the flying dipole’s relation, and (3) the interaction is suppressed at high energy-momentum by a nonanalytic damping factor. According to the flying dipole’s relation, interaction among the noncommutative dipoles, if exists, ought to obey geometric constraints among the dipole moments. An outstanding question would then be building up an intuitive picture of the interaction, which we try to answer in this work. The main results assert that cubic interaction among the open

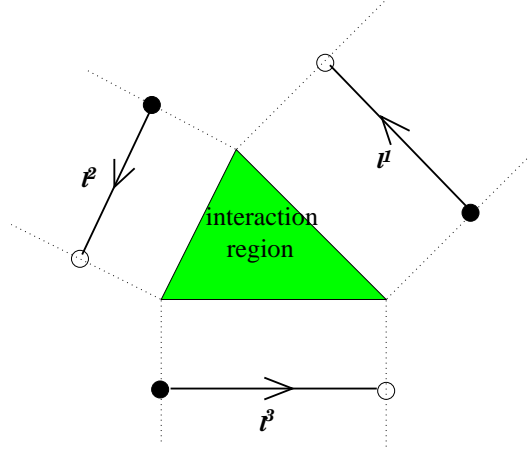


Figure 2: *Interaction of three noncommutative dipoles. At interaction region, the dipoles are expected to interact locally pairwise.*

Wilson lines is governed by a remarkably simple effective action, schematically taking the following form:

$$\Gamma_3[W] = \frac{\lambda_c}{3!} \text{Tr}_{\mathcal{H}_{\text{dipole}}} \mathbf{K}_3 \left(\widehat{W} \star \widehat{W} \star \widehat{W} \right) \quad \text{where} \quad \lambda_c = (\lambda/2)^2. \quad (1.4)$$

Here, \mathbf{K}_3 represents a weight-factor over \mathcal{H} , and the $\hat{\star}$ -product refers to a newly emergent noncommutative algebra obeyed by the open Wilson lines as ‘closed strings’.

This paper is organized as follows. In section 2, we rederive the one-loop effective action [9, 10] via the saddle-point method. In section 3, starting from two-loop Feynman diagrammatics, we obtain factorized expression of the two-loop effective action. In section 4, we evaluate the effective action via saddle-point method and show emergence of snapped open Wilson lines. In section 5, we obtain the proclaimed result Eq.(1.4).

2 One-loop Effective Action Revisited

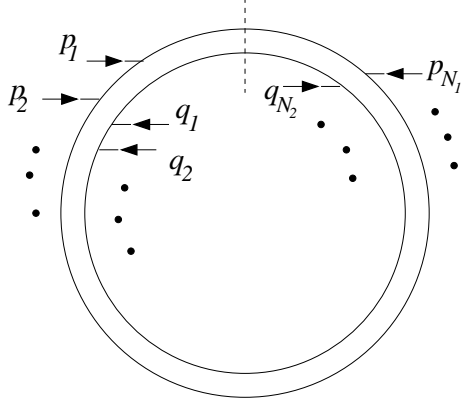


Figure 3: One-loop Feynman diagram for N-point Green function. There are N_1 and N_2 -insertions of external momenta along the inner and outer boundary of the Feynman diagram in double line notations.

We first recapitulate aspects of the one-loop effective action [9, 10] relevant for discussion in later sections. The effective action is defined as

$$\Gamma_{1\text{-loop}} = \sum_{N=0}^{\infty} \frac{1}{N!} \Gamma_N,$$

viz. a sum over N-point, one-particle-irreducible Green function, Γ_N :

$$\Gamma_N[\{p_i\}, \{q_j\}] = \hbar \left(-\frac{\lambda}{2} \right)^N \sum_{N_1+N_2=N} \frac{C_{\{N\}}}{(4\pi)^{d/2}} \int_0^\infty \frac{dT}{T} T^{-\frac{d}{2}+N} \exp \left[-m^2 T - \frac{\ell^2}{4T} \right] J_{N_1}(\ell) J_{N_2}(-\ell).$$

Here, we have denoted N-dependent combinatoric factor as $C_{\{N\}}$, divided N external momenta into two groups: $\{p_1, \dots, p_{N_1}\}$ and $\{q_1, \dots, q_{N_2}\}$, and defined $k = \sum_{i=1}^{N_1} p_i = -\sum_{i=1}^{N_2} q_i$, and $\ell := \theta \cdot k$ (consistent with the flying dipole's relation). We have also defined a kernel $J_{N_1}(\ell)$ by

$$J_{N_1}(\ell, \{p_i\}) := \int_0^1 \cdots \int_0^1 d\tau_1 \cdots d\tau_{N_1} \exp \left[-i \sum_{i=1}^{N_1} \tau_i p_i \cdot \ell - \frac{i}{2} \sum_{i < j=1}^{N_1} \epsilon(\tau_{ij}) p_i \wedge p_j \right] \quad (2.1)$$

in which $\tau_i \sim \tau_i + 1$, ($i = 1, 2, \dots$) denote moduli parameter for i -th marked point around a boundary of the vacuum diagram, where a background field Φ with momentum p_i is inserted, and $\tau_{ij} := (\tau_i - \tau_j)$. Similarly, $J_{N_2}(-\ell, \{q_j\})$ is defined around the other boundary of the vacuum diagram. Eq.(2.1) is precisely momentum-space representation of the \star_N -product, originally introduced in [12, 13]².

²As $k \cdot \ell = 0$, the kernel is invariant under a uniform shift of all moduli parameters: $\tau_i \rightarrow \tau_i + (\text{constant})$. Using the invariance, one can shift the τ -integral domain in Eq.(2.1) to $[-1/2, +1/2]$. This choice is preferred, as it displays Hermiticity property of J_N manifestly.

In the large noncommutative limit, $\theta^{mn} \rightarrow \infty$ (compared to typical energy-momentum scale), the T-moduli integral is evaluated accurately via the saddle-point method. Clearly, the saddle-point is located at $T = |l|/2m$. Moreover, the leading-order correction is from Gaussian integral over the quadratic variance in the exponent, and is easily computed to be $(\pi|l|/m^3)^{1/2}$. Thus, putting all these pieces together, the one-loop, N-point Green function is obtained as

$$\begin{aligned} \Gamma_N[\{p_i\}, \{q_j\}] &= \hbar(4\pi)^{-\frac{d}{2}} \left(\frac{|l|}{2m}\right)^{-\frac{d}{2}} \left(\frac{2\pi}{m|l|}\right)^{1/2} e^{-m|l|} \\ &\times \sum_{N_1+N_2=N} C_{\{N\}} \left\{(-g)^{N_1} |l|^{N_1} J_{N_1}(\ell)\right\} \left\{(-g)^{N_2} |l|^{N_2} J_{N_2}(-\ell)\right\}, \quad (2.2) \end{aligned}$$

where $g := (\lambda/4m)$. The factorized expression permits resummation of the double-sum over N_1 and N_2 . Indeed, taking carefully into account of the combinatorial factors $C_{\{N\}} = \frac{1}{2}(N!/N_1!N_2!)$, we find that each factor involving the \star_N -kernel J_N 's are exponentiated into the *scalar* open Wilson lines. Convoluting the Green functions with the background Φ -fields and summing over N , the result is

$$\Gamma_{1\text{-loop}}[W(\Phi)] = \frac{\hbar}{2} \int \frac{d^d k}{(2\pi)^d} W_k[\Phi] \mathcal{K}_{-\frac{d}{2}}(|l|) W_{-k}[\Phi].$$

Here,

$$\mathcal{K}_{-\frac{d}{2}}(|l|) = \left(2\pi \frac{|l|}{m}\right)^{-\frac{d}{2}} \left(\frac{2\pi}{m|l|}\right)^{1/2} e^{-m|l|}$$

denotes the propagation kernel of the noncommutative dipole, accounting for the UV-IR mixing and infrared singularity at $\ell \rightarrow 0$, and

$$\begin{aligned} W_k[\Phi] &= \sum_{N=0}^{\infty} \frac{1}{N!} (-g|l|)^N \int \frac{d^d p_1}{(2\pi)^d} \cdots \int \frac{d^d p_N}{(2\pi)^d} (2\pi)^d \delta^d(p_1 + \cdots + p_N - k) \\ &\times [J_N(\ell, \{p_i\}) \cdot \tilde{\Phi}(p_1) \cdots \tilde{\Phi}(p_N)] \quad (2.3) \end{aligned}$$

denotes the *scalar* open Wilson line operator, expressed as a convolution of the \star_N -product kernel J_N , Eq.(2.1) [9, 13, 14].

Note that, inferred from the general expression, Eq.(1.3), saddle-point contour of the open Wilson line Eq.(2.3) is a straight line: $y^m(\tau) = \theta^{mn} k_n \tau$, thus mapping compact τ -moduli space (of topology \mathbf{S}^1 , corresponding to each of the two boundaries in Fig.(3) to a straight line of interval ℓ in spacetime. Obviously, such straight open Wilson lines obey the ‘flying dipole relation’ Eq.(1.1). The contour will begin to fluctuate, however, once contributions beyond the saddle-point are taken into account, yielding plethora of higher-mode excitations. In the rest of this paper, we will see that, at higher-loops, even the saddle-point contour turns out different from a straight line.

3 Two-Loop Effective Action

3.1 Two-Loop Green Functions

Begin with the two-loop nonplanar contribution to the N -point one-particle-irreducible Green functions. The general expression of these Green functions have been obtained recently in [15] using the worldline formulation approach³. The result agrees with that obtainable from the noncommutative Feynman diagrammatics, which we shall be presenting in Appendix A, and is given by:

$$\Gamma_N(\{p_a^{(a)}\}) = \frac{\hbar^2 \lambda^2}{24} \left(-\frac{\lambda}{2}\right)^N \sum_{N_1, N_2, N_3=0}^N \sum_{\{\nu\}} (2\pi)^d \delta \left(\sum_{a=1}^3 \sum_{n=1}^{N_a} p_n^{(a)} \right) C_{\{N\}} \Gamma_\nu^{(N_1, N_2, N_3)}. \quad (3.1)$$

Here, $C_{\{N\}}$ denotes a combinatoric factor (see section 4.2), and

$$\begin{aligned} \Gamma_\nu^{(N_1, N_2, N_3)} &= \frac{1}{(4\pi)^d} \int_0^\infty \cdots \int_0^\infty dT_1 dT_2 dT_3 e^{-m^2(T_1+T_2+T_3)} \Delta^{\frac{d}{2}}(T) \left(\prod_{a=1}^3 \int_0^{T_a} \prod_{i=1}^{N_a} d\tau_i^{(a)} \right) \\ &\times \exp \left[\frac{1}{2} \sum_{i,j=1}^N p_i \cdot G^{(0)} \cdot p_j \right] \exp \left[-\frac{1}{4} \Delta(T) \sum_{a=1}^3 T_a k_a \circ k_a \right] \\ &\times \exp \left[-\frac{i}{2} \sum_{a=1}^3 \left(P_a^- \wedge P_a^+ + \frac{1}{3} P_a \wedge P_{a+1} \right) \right] \\ &\times \exp \left[-\frac{i}{4} \sum_{k < \ell}^{N_a} \left(\nu_k^{(a)} + \nu_\ell^{(a)} \right) \epsilon \left(\tau_{k\ell}^{(a)} \right) p_k^{(a)} \wedge p_\ell^{(a)} \right] \\ &\times \exp \left[i \Delta(T) \sum_{a=1}^3 T_a k_a \wedge \left(\sum_{i=1}^{N_{a+2}} \tau_i^{(a+2)} p_i^{(a+2)} - \sum_i^{N_{a+1}} \tau_i^{(a+1)} p_i^{(a+1)} \right) \right], \end{aligned} \quad (3.2)$$

in which

$$\Delta(T) := (T_1 T_2 + T_2 T_3 + T_3 T_1)^{-1}. \quad (3.3)$$

This is the main result, which we will take as the starting point for the analysis in later sections. In the rest of this subsection, we explain our notations in Eqs.(3.1, 3.2, 3.3). Derivation of Eq.(3.1) via the noncommutative Feynman diagrammatics will be relegated to Appendix A.

The Feynman diagram under consideration is depicted in Fig.4. We construct the *planar* two-loop vacuum diagram⁴ by Wick-contracting two $\lambda[\Phi^3]_\star$ -interaction vertices

³For recent study of multiloop Φ^3 -theory amplitudes from string theory, see [16].

⁴At two loop and beyond, vacuum diagrams are classifiable into a planar diagram and the rest, nonplanar diagrams. If the number of twist insertion is zero, the vacuum diagram is referred as planar. All other vacuum diagrams, with at least one insertion of the twist, are nonplanar ones. At one loop, by default, the vacuum diagram is planar.

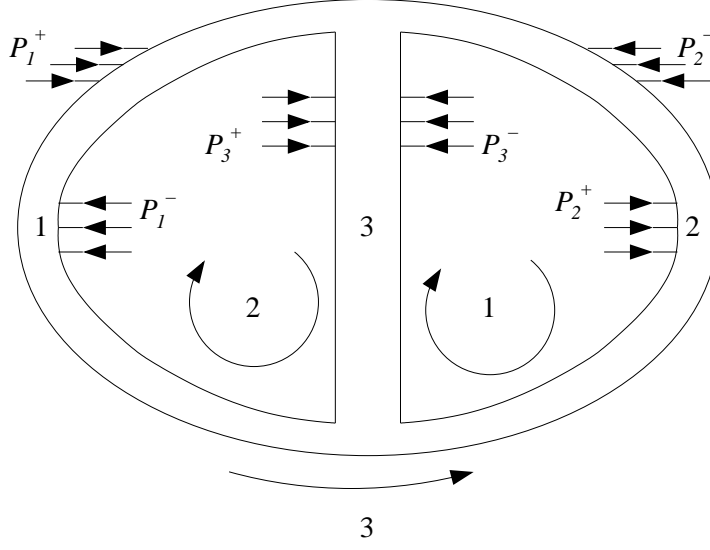


Figure 4: Two-loop Feynman diagram for N -point Green function. Note that we have labelled the legs and the vacuum diagram boundaries dual to each other. The external momenta $p_i^{(a)}$, Feynman-Schwinger moduli parameters $\tau_i^{(a)}$, and Moyal's phase-factor signs $\nu_i^{(a)}$ are ordered from top to bottom, viz., $p_1^{(a)}$ refers the closest interaction vertex to the top, then $p_2^{(a)}$, and so on. With this ordering convention, the τ 's are ranging over $0 < \tau_N < \dots < \tau_1 < T$ for each connected side of the three internal propagators.

via three internal propagators. Label the propagators as $a = 1, 2, 3$ and draw them in double-line notation, as is natural for noncommutative field theories. Moduli parameters T_1, T_2, T_3 refer to the Feynman-Schwinger parameters of the three internal propagators, and range over the moduli space of two-loop vacuum Feynman diagram: $\mathcal{M}_{2\text{-loop}} = [0, \infty) \otimes [0, \infty) \otimes [0, \infty)$. On the vacuum Feynman diagram, we mark N points at locations $\tau_i^{(a)}$, where $a = 1\pm, 2\pm, 3\pm$ and $i = 1, 2, \dots, N_a$, and insert background Φ -fields. Each group of the Φ -field insertions is classifiable into those affixed from the inner and the outer boundaries. Sum over all possible insertion of the external lines is given by integration over the moduli parameters $\tau_i^{(a)}$'s over $[0, T_a]$, and $\tau_{ij}^{(a)}$ refers to $(\tau_i^{(a)} - \tau_j^{(a)})$.

Momenta of background Φ -fields attached at a -th internal propagator are labelled as $\{p_i^{(a)}\}$, where $a = 1, 2, 3$ and $i = 1, 2, \dots, N_a$. Total momentum injected on the a -th internal propagator is denoted as:

$$P_a^\pm \equiv \sum_{i=1}^{N_a} \frac{1 \pm \nu_i^{(a)}}{2} p_i^{(a)} \quad \text{and} \quad P_a \equiv P_a^+ + P_a^-, \quad (3.4)$$

where \pm refers to the 'left' and the 'right' sides of a -th boundary (see Fig.4), respectively, and $\nu_i^{(a)}$ takes ± 1 depending on whether the background Φ -field is attached from the 'left' or the 'right' side of the double-lined internal propagator. We have also introduced the

total momentum inserted on each *worldsheet boundary* via

$$k_{a+2} = P_a^+ + P_{a+1}^- . \quad (3.5)$$

Various products in Eq.(3.2) are defined as follows:

$$A \cdot B := \delta^{mn} A_m B_n, \quad A \wedge B := \theta^{mn} A_m B_n, \quad A \circ B := \delta_{mn} (\theta \cdot A)^m (\theta \cdot B)^n.$$

In this paper, following [9], we work exclusively in the limit of low energy-momentum, large noncommutativity, and weak external field:

$$p_i^{(a)}/m = \mathcal{O}(\epsilon^{+1}), \quad m^2 \theta^{mn} = \mathcal{O}(\epsilon^{-2}), \quad \text{and} \quad \lambda \Phi / m^2 = \mathcal{O}(\epsilon^{+1}) \quad \text{as} \quad \epsilon \rightarrow 0^+. \quad (3.6)$$

The first two limits ensure that various energy-momentum products in the exponent of Eq.(3.2) are hierarchically separated as

$$p_i^{(a)} \cdot p_j^{(b)} T \ll p_i^{(a)} \wedge p_j^{(b)} \ll m^2 T \sim p_i^{(a)} \circ p_j^{(b)} / T, \quad (3.7)$$

at the saddle-point value, $T \sim \ell/2m$, we will eventually find. As shown in [9, 10] and reviewed in section 2, the limit Eq.(3.6) and the relation Eq.(3.7) simplified computation of the one-loop effective action enormously. The third limit of Eq.(3.6), viz. the weak external field limit, also simplifies the moduli-space integral. Schematically, the integral is given by

$$\int_0^\infty \frac{dT}{T} T^{-\frac{d}{2}} \exp \left(-m^2 T - \frac{\ell^2}{4T} \right) \sum_{N=0}^\infty \frac{1}{N!} T^N (-\lambda \Phi)^N ,$$

and appears that the saddle-point approximation might break down for the summand of large N . The sum over N , however, is estimated $\mathcal{O}(e^{-T\lambda\Phi})$, and hence is negligible once the third limit in Eq.(3.6) is taken. We note that the exponent of the open Wilson line ($\sim e^{-\lambda\ell\Phi/m}$) still remains of $\mathcal{O}(1)$ in the limit Eq.(3.6). The same limit Eq.(3.6) will be taken in computing the two-loop effective action, and will turn out to yield considerable simplification, far more remarkable than in the one-loop computation.

For later convenience, we refer to the last three exponential terms in Eq.(3.2), involving \wedge -product, as Ξ_1, Ξ_2, Ξ_3 , respectively. At this point, it suffices to note that Ξ_1 is *independent* of the moduli parameters $\tau_i^{(a)}$'s, Ξ_2 depends on the *ordering* of the moduli parameters, and the exponent of Ξ_3 depends *linearly* on the moduli parameters.

3.2 Factorization

As is well-known, the one-particle-irreducible diagrams in field theories are derivable from connected diagrams in string theory (see [17] for an example in the two-loop context). The

open string theory diagrams are labelled by external momenta of vertex operators inserted along the worldsheet boundaries, with a fixed cyclic ordering on each boundary, but are otherwise insensitive to details of the momentum distribution on a given boundary. On the other hand, according to the steps leading to Eq.(3.2), the field theory diagrammatics appear to distinguish, in Fig.(4), the different parts of a given boundary. Specifically, whereas the worldsheet boundary momenta are k_a 's, the Feynman diagrammatics Eq.(3.2) is expressed in terms of individual P_a^\pm 's. See Eq.(3.5).

Can we reorganize a collection of Feynman diagrams belonging to the same graph-theoretic combinatorics and simplify them so that the correspondence to the string theory diagram becomes manifest? The answer is affirmatively positive. Steps leading to the answer are as follows. First, both the local phase-factor in Ξ_2 and the τ -dependent phase-factor in Ξ_3 are readily splitted into three parts, each of which is attributable to the three boundaries, as depicted in Fig.(4). Second, utilizing the overall energy-momentum conservation $P_1 + P_2 + P_3 = 0$, the τ -independent phase-factor in Ξ_1 is re-expressible as:

$$\Xi_1 = \exp \left[-\frac{i}{2} \sum_{a=1}^3 \left(P_a^+ \wedge P_{a+1}^- + \frac{1}{3} k_a \wedge k_{a+1} \right) \right] .$$

The first term consists of \wedge -product among partial momenta carried by the two halves of each boundary, whereas the second term depends only on the net momenta carried by each boundary. Reorganizing this way, the last three exponentials in Eq.(3.2) are factorizable in the following way:

$$\Xi_1 \Xi_2 \Xi_3 = \prod_{a=1}^3 \left(\Xi_1^a \Xi_2^a \Xi_3^a \right) \times \exp \left[-\frac{i}{2} \sum_{a=1}^3 \frac{1}{3} k_a \wedge k_{a+1} \right] , \quad (3.8)$$

$$\Xi_1^a = \exp \left[-\frac{i}{2} P_{a+1}^+ \wedge P_{a+2}^- \right] , \quad (3.9)$$

$$\Xi_2^a = \exp \left[-\frac{i}{2} \left(\sum_{i < j} p_i \wedge p_j \epsilon(\tau_{ij}) \right)^{(a+1)+} + \frac{i}{2} \left(\sum_{i < j} p_i \wedge p_j \epsilon(\tau_{ij}) \right)^{(a+2)-} \right] , \quad (3.10)$$

$$\begin{aligned} \Xi_3^a &= \exp \left[-i \Delta(T) \left(\sum \tau p \right)^{(a+1)+} \wedge (T_{a+2} k_{a+2} - T_a k_a) \right] \\ &\times \exp \left[-i \Delta(T) \left(\sum \tau p \right)^{(a+2)-} \wedge (T_a k_a - T_{a+1} k_{a+1}) \right] . \end{aligned} \quad (3.11)$$

A remark is in order. Consider, for instance, along the $(a = 3)$ boundary, making a move of an external Φ -field line from the $(1+)$ side to the $(2-)$ side while preserving the cyclic ordering. Clearly, each component of the exponentials $\Xi_{1,2,3}^3$ makes a jump when the line crosses the borders between $(1+)$ and $(2-)$ sides. It turns out that, for both for the top and the bottom borders, the jump cancels out. That is, for all cyclically ordered background Φ -field insertions along each boundary, the phase-factors $\Xi_1 \Xi_2 \Xi_3$ are

continuous and periodic as the insertion moduli τ 's are varied. This is, of course, what one expects from underlying string theory diagrams.

We now rescale the moduli parameters as $\tau^{(a\pm)} \rightarrow \mp \tau^{(a\pm)} T_a$. Then, τ runs over $[-1, 0]$ for the points on the (+) side, and over $[0, +1]$ for the points on the (-) side, where the two sides belong to the same worldsheet boundary. The sign flip on the (+) side amounts to aligning the two integration regions in the same direction around the oriented worldsheet boundary: $\int_0^1 d\tau^{(a+)} \rightarrow \int_{-1}^0 d\tau^{(a+)}$ renders the τ -moduli increment on the (+) side coincide with the worldsheet boundary direction shown in Fig.(4). Suppose the background Φ -fields are inserted N_1^+ and N_2^- times on the (1+) and (2-) sides of the ($a = 3$) boundary, respectively. After the aforementioned redefinition of τ 's, the Ξ_1^3 and Ξ_2^3 are combined to ⁵

$$\Xi_1^3 \Xi_2^3 = \exp \left[+\frac{i}{2} \sum_{i < j=1}^{N_1^+ + N_2^-} p_i \wedge p_j \epsilon(\tau_{ij}) \right]. \quad (3.12)$$

Furthermore, Ξ_3^3 is simplifiable considerably as

$$\Xi_3^3 = \exp \left[-i \sum_{i=1}^{N_1^+} (\tau p_i)^{(1+)} \cdot (-\alpha_1) - i \sum_{i=1}^{N_2^-} (\tau p_i)^{(2-)} \cdot (+\alpha_2) \right]. \quad (3.13)$$

Here, α 's are vectors formed out of the dipole moments $\{\ell_a\}$ via

$$\alpha_1 = t_1(t_2 l_2 - t_3 l_3), \quad \alpha_2 = t_2(t_3 l_3 - t_1 l_1), \quad \alpha_3 = t_3(t_1 l_1 - t_2 l_2). \quad (3.14)$$

$$t_a = \sqrt{\Delta} T_a \quad \text{where} \quad (t_1 t_2 + t_2 t_3 + t_3 t_1) = 1. \quad (3.15)$$

The overall energy-momentum conservation, $k_1 + k_2 + k_3 = 0$, puts the three dipole vectors $\{\ell_a\}$ form a triangle, referred as 'dipole-triangle'. Geometrically, for non-negative values of $\{t_a\}$, the vectors $\{\alpha_a\}$ in Eq.(3.14) split the 'dipole-triangle' into three pieces (See Fig. 5), viz.

$$l_1 = \alpha_3 - \alpha_2, \quad l_2 = \alpha_1 - \alpha_3, \quad l_3 = \alpha_2 - \alpha_1. \quad (3.16)$$

Observe now that, after the factorization, exponentials in Eq.(3.12) and Eq.(3.13) are altogether strikingly reminiscent of the \star_N -product kernel, Eq.(2.1), encountered at one-loop computation! As we will see shortly, they are resumable into a scalar open Wilson

⁵ Precisely the same construction goes through for $a = 1, 2$ boundaries, and the derivation will be omitted.

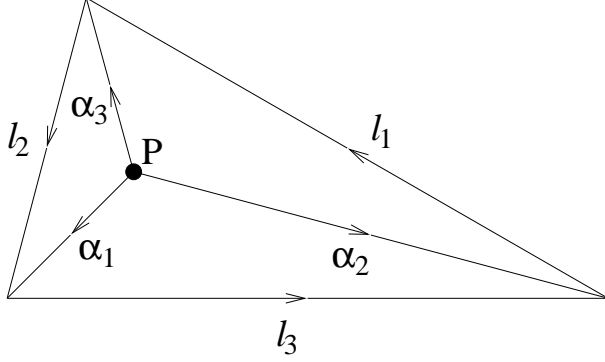


Figure 5: Due to momentum conservation ($k_1 + k_2 + k_3 = 0$), the vectors l_1, l_2, l_3 form a triangle. For any given value of the normalized moduli $\{t_a\}$, the α 's split the triangle into three pieces. The saddle point conditions in Section 4 demand that the angle between a pair of α 's is $2\pi/3$.

line whose contour is not a straight line but a snapped wedge. Thus, introduce the two-loop \star_N -product kernel as ⁶

$$\hat{J}_{(N_1^+, N_2^-)}(-\alpha_1, \alpha_2) = \prod_{i=1}^{N_1^+} \int_{-1}^0 d\tau_i^{(1+)} \prod_{j=1}^{N_2^-} \int_0^{+1} d\tau_j^{(2-)} \Xi_1^{(3)} \Xi_2^{(3)} \Xi_3^{(3)} \quad \text{for } a = 3, \quad (3.17)$$

and, similarly, $\hat{J}_{(N_2^+, N_3^-)}(-\alpha_2, +\alpha_3)$, $\hat{J}_{(N_3^+, N_1^-)}(-\alpha_3, +\alpha_1)$ for $a = 1$ and 2 , respectively.

We have denoted the two-loop kernels \hat{J} 's hatted in order to emphasize functional difference of them from the one-loop kernel J 's. Nevertheless, the two are intimately related each other. To see this, use the identity $t_1 t_2 + t_2 t_3 + t_3 t_1 = 1$, and split the exponential term in Eq.(3.8) into three parts:

$$\exp \left[-\frac{i}{2} t_2 t_3 k_2 \wedge k_3 \right] \exp \left[-\frac{i}{2} t_3 t_1 k_3 \wedge k_1 \right] \exp \left[-\frac{i}{2} t_1 t_2 k_1 \wedge k_2 \right].$$

Permutation symmetry among the three exponentials suggests that each exponential is attachable to the three \hat{J} 's for $a = 1, 2, 3$. Indeed, using the identity

$$P_1^+ \wedge P_2^- + t_1 t_2 k_1 \wedge k_2 + P_1^+ \cdot \alpha_1 + P_2^- \cdot \alpha_2 = 0,$$

derivable from the overall energy-momentum conservation, one can show readily that the \hat{J} 's in Eq.(3.17) satisfies the following decomposition rule:

$$\hat{J}_{(N_1^+, N_2^-)}(-\alpha_1, \alpha_2) = \exp \left[\frac{i}{2} t_1 t_2 k_1 \wedge k_2 \right] J_{N_1^+}(-\alpha_1) J_{N_2^-}(\alpha_2), \quad (3.18)$$

where J 's are to be understood as Eq.(2.1) but with the domain of moduli integrals shifted to $[-1/2, +1/2]$. Thus, the two-loop \star_N -product kernel is decomposable into a

⁶ How they are related to the \star_N -products and the scalar open Wilson lines will be elaborated in the next section.

product of two, one-loop \star_N -product kernels. A notable feature of the decomposition is that the product among the one-loop kernels is not an ordinary product, but is a sort of (moduli-dependent) Moyal product. Moreover, decomposed as in Eq.(3.18), the \hat{J} 's display Hermiticity property manifestly — with the integral domain shifted to $[-1/2, +1/2]$, each of the two one-loop kernels in Eq.(3.18) is manifestly Hermitian, and, under Hermitian conjugation and interchange between $1 \leftrightarrow 2$, the newly emergent Moyal product on the right-hand-side of Eq.(3.18) remains unchanged.

4 Two-Loop Moduli Space Integral

4.1 Saddle-Point Analysis

We now perform, in Eq.(3.2), the integration over T_1 , T_2 and T_3 , viz. moduli space of the two-loop, planar, *vacuum* Feynman diagram. Here enters the utility of the limit Eq.(3.6), as the integration is simplified considerably. Specifically, (1) the low energy limit, $p_i^{(a)} \cdot p_j^{(b)} \ll m^2$, permits to drop the first exponential in Eq.(3.2), (2) the large noncommutativity, $m^2 T \sim k_a \circ k_a / T$, permits to evaluate the integrals via the saddle-point method, and (3) the weak field limit, $\lambda \Phi \ll m^2$, permits to drop, in the saddle-point analysis, contribution of power-series in $(\lambda \Phi T)$. We will find that, as a result of these simplifications, a version of open Wilson lines emerges naturally as the saddle-point configuration.

We begin with detailed consideration of the moduli space integral. The integral is decomposable, via the change of variables Eq.(3.15), into one-dimensional integral over the ‘size’ $\Delta(T)$, and two-dimensional integral over the ‘angles’ t_1, t_2, t_3 (subject to the constraint $(t_1 t_2 + t_2 t_3 + t_3 t_1) = 1$). The decomposition is suited the most for the saddle-point analysis, as the $\Xi_{1,2,3}^{(a)}$ are independent of the ‘size’ $\Delta(T)$, which is evident from Eqs.(3.12, 3.13) and the definition of α 's in Eq.(3.14). Domain of the moduli space in these variables is readily identifiable. Evidently, the ‘size’ variable ranges over $\Delta = [0, \infty)$. For the ‘angle’ variables, using Eq.(3.14), one can map their range to the range of the α -vectors. The latter is seen equal to the *interior* of the ‘dipole-triangle’ formed out of the three dipole moments, $\{\ell_a\}$: as the ‘angle’ variables are varied, the junction point P of the three α vectors sweeps out the ‘dipole-triangle’ exactly once. See Fig.(5).

We now identify saddle-point value of $\Delta(T)$ and saddle-point location of P , and compute the dominant contribution to the moduli space integral. Specifically, for the saddle-point analysis, take the following part of the integrand only:

$$\exp F(T_1, T_2, T_3) := \exp \left[-m^2 (T_1 + T_2 + T_3) - \frac{1}{4} \Delta(T) (T_1 l_1^2 + T_2 l_2^2 + T_3 l_3^2) \right], \quad (4.1)$$

viz. the part dependent on the ‘size’ variable. The saddle-point conditions, $(\partial F/\partial T_a) = 0$, are then expressible, in terms of the ‘polar’ variables, as

$$\Delta(T) = \frac{4m^2}{L^2} \quad (4.2)$$

and

$$L \equiv |t_1 l_1 - t_2 l_2| = |t_2 l_2 - t_3 l_3| = |t_3 l_3 - t_1 l_1|. \quad (4.3)$$

Geometrically, the ‘size’ condition Eq.(4.2) fixes $\Delta(T)$ in terms of the area of the ‘dipole-triangle’ (which grows large in the large noncommutativity limit), while the ‘angle’ condition Eq.(4.3) puts the inner-angle between two adjacent α ’s to $(2\pi/3)$ ⁷. The saddle-point is thus located at

$$T_a = \Delta^{-1/2}(T) t_a = \frac{L}{2m} t_a = \frac{|\alpha_a|}{2m}, \quad (4.4)$$

for which the saddle-point value of the exponent

$$F(\text{saddle-point}) = -m(|\alpha_1| + |\alpha_2| + |\alpha_3|)|_{\text{saddle-point}} \quad (4.5)$$

is geometrically a linear sum of lengths of the three vectors, $\{\alpha_a\}$. As we will show in the next subsections, simple geometric description of the saddle-point Eq.(4.4) permits the two-loop effective action expressible entirely in terms of the scalar open Wilson lines.

We close the saddle-point analysis with a few remarks that warrant further technical elaboration. First, as in the one-loop computation in Section 2, one can perform the moduli integrals beyond the saddle-point, Eq.(4.5). The leading-order correction is from quadratic variance of $F(T)$ in the neighborhood of the saddle-point, and, upon Gaussian integral, yields a pre-exponential correction, denoted as $(\Delta_F)^{-3/2}$. In Appendix C, we compute $(\Delta_F)^{-3/2}$ and find that it also admits a simple geometric interpretation. Second, in setting up the saddle-point analysis, one might be concerned with potential contribution to Eq.(4.1) from angular variation, viz. t -dependent, \wedge -product part. Fortunately, in the large noncommutativity limit Eq.(3.6), the angle-dependent part drops out of the analysis. To illustrate this, consider evaluating the moduli integrals over (Δ, t_1, t_2) via the saddle-point analysis. Recall that the \wedge -product part is independent of Δ , and hence does not affect the Δ integral. Thus, after the Δ -integral, we are left with

$$\int d^2 t e^{-m L f(t)} g(t),$$

where $f(t)$ refers to a dimensionless function of t , whose saddle-point t^* is determined by Eq.(4.3). The function $g(t)$ includes the \hat{J} part (the \wedge -product part) and powers of

⁷In Appendix A, we solve these saddle-point conditions and determine explicitly the saddle-point value of $\{t_a\}$ in terms of the dipole moments $\{\ell_a\}$.

t . From the expression, one readily finds that the function $g(t)$ and its derivatives are of $\mathcal{O}(1)$. Taylor-expanding $g(t)$ around t^* , a simple power-counting reveals that the n -th order term is suppressed by a factor of $(mL)^{-n/2}$. Hence, in the limit $mL \gg 1$ we are working with, the function $g(t)$ does not affect the saddle-point analysis based solely on the function $e^{-mLf(t)}$.

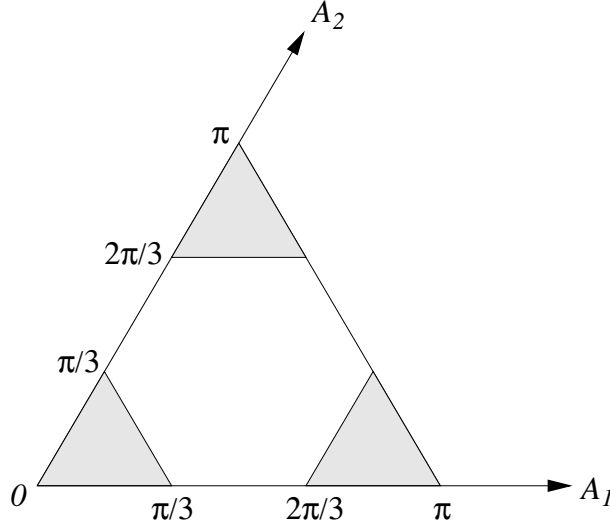


Figure 6: *Moduli space of the ‘dipole-triangle’.* A point in the moduli space represents a particular shape of the dipole-triangle (defined up to size) whose two angles, A_1, A_2 , are the coordinates of the point. Three corner regions are shaded.

Third, a simple geometric consideration reveals that the ‘ $(2\pi/3)$ -condition’, Eq.(4.3), is violated if any of the inner-angles in the ‘dipole-triangle’ exceeds $2\pi/3$. Consider the moduli space of all possible ‘dipole-triangle’ is depicted in Fig.(6), where it is divided into a central region and three corner regions. The previous saddle-point analysis is valid in the central region. In the corner regions, where one of the three inner-angles in the ‘dipole-triangle’ exceeds $2\pi/3$, the saddle-point analysis breaks down. For instance, if the inner-angle between l_1 and l_2 is bigger than $2\pi/3$, the naive saddle-point analysis yields a negative value of T_3 at the saddle-point, and hence the point P lies outside the ‘dipole-triangle’. As the moduli integrals cover only the positive values of T_a , we will have to devise an another approximation method. This turns out to be straightforward. In the lower-left corner region of Fig.(6), one can evaluate the T_1 and T_2 integrals, still utilizing the saddle-point method. The remaining T_3 integral is then schematically of the form:

$$\int dT_3 e^{-m^2 T_3 T_3^{N_3}} \sim m^{-2N_3},$$

which eventually leads to the resummation

$$\sum_{N_3} \frac{1}{N_3!} \left(-\frac{\lambda\Phi}{m^2} \right)^{N_3}.$$

Thanks to the weak field limit, $\lambda\Phi/m^2 \ll 1$ in Eq.(3.6), we can safely keep the leading-order, $N_3 = 0$ term only, viz. set the entire resummation to be unity. As this renders no insertion of the background Φ -field on the $a = 3$ internal propagator, it sets $P_3^+ = P_3^- = 0$. It turns out that the rest of the saddle-point method is applicable and the geometric structure does not change, except that now $\alpha_3 = 0$, $\alpha_2 = -\ell_1$ and $\alpha_1 = \ell_2$. In the other two corner regions in Fig.(6), the same analysis holds regarding T_1, T_2 integrals and ensures no-insertion of the background Φ -field on $a = 1, 2$ internal propagators. A noteworthy point is that these three corners of the moduli space correspond in the two-loop vacuum Feynman diagrammatics to the degeneration limit where one of the three internal propagators is shrunk to a zero length. If the moduli space is extended to accomodate ‘topology change’ across the three corners, the resulting diagrams are one-particle-*reducible*, dumb-bell shaped Feynman diagram. Intriguingly, after a straightforward computation, we were able to show that, functionally, these one-particle-reducible diagrams are smoothly connected to the diagrams at the three corners as T_a ’s are extended to negative values. It implies that, within the saddle-point analysis, one might take an alternative viewpoint that effective field theory of noncommutative dipoles originate not just from one-particle-irreducible diagrams but also one-particle-reducible ones. Needless to say, it is tantalizingly reminiscent of the worldsheet diagrammatics in string theory.

4.2 Combinatorics

We next add up Feynman diagrams with different combinatorics of background Φ -field insertion, and obtain the two-loop effective action. In Eq.(3.2), the summations

$$\sum_{N_1+N_2+N_3=N} \sum_{\{\nu\}}$$

are over all possible insertion of total N background Φ -fields; each a -th internal propagator carries N_a out of them (with all possible orderings, as τ ’s run from 0 to 1 independently). The sign-factor $\nu_i^{(a)}$ keeps track of whether a given Φ -field is attached on the left or the right side of the propagator. In the commutative setup, the left/right insertions are not distinguished, and hence the summands consist of 3^N combinatorically distinct diagrams. In the noncommutative case, the inclusion of the last summation makes the total number of summands into 6^N . Note also the important point that the coupling parameter for background Φ -field insertion is rescaled as $\lambda \rightarrow \lambda/2$ in the noncommutative case.

The two-loop Green functions Eq.(3.2) were originally sorted out by how the Φ -field insertions are distributed among three internal propagators. However, the result of the last section suggests that we ought to sort out the Green functions according to the way the Φ -field insertions are distributed among three *boundaries*. Thus, we decompose the diagrams according to the combinatorics

$$6^N = (2 + 2 + 2)^N = \sum_{\sum N_i = N} \frac{N!}{M_1!M_2!M_3!} \left(\frac{M_1!}{N_2^+!N_3^-!} \right) \left(\frac{M_2!}{N_3^+!N_1^-!} \right) \left(\frac{M_3!}{N_1^+!N_2^-!} \right).$$

In the summation, N_a^\pm are the number of momenta inserted on the (\pm) -side of a -th internal propagator, and $M_a = (N_{a+1}^+ + N_{a+2}^-)$ is the total number of momenta on the a -th boundary.

Specifically, the combinatoric factors organize the summation of the two-loop effective action in the following simple manner:

$$\begin{aligned} \Gamma &= \sum_N \frac{1}{N!} \Gamma_N \\ \Gamma_N &= \sum_{\{M_a\}} \frac{N!}{M_1!M_2!M_3!} \Gamma_{(M_1, M_2, M_3)} \quad \text{where} \quad (M_1 + M_2 + M_3) = N \end{aligned}$$

and

$$\begin{aligned} \Gamma_{(M_1, M_2, M_3)} &= \prod_a \Gamma_{M_a}^{(a)} \\ \Gamma_{M_a}^{(a)} &= \sum_{N_{a+1}^+, N_{a+2}^-} \frac{M_a!}{N_{a+1}^+!N_{a+2}^-!} \Gamma_{N_{a+1}^+, N_{a+2}^-}^{(a)} \quad \text{where} \quad (N_{a+1}^+ + N_{a+2}^-) = M_a. \end{aligned}$$

As shown in section 3, $\Gamma_{N_{a+1}^+, N_{a+2}^-}^{(a)}$ contains in its integrand, after Wick rotation back to Minkowski signature, terms of the combination:

$$\left(-\frac{\lambda}{2} \right)^{N_{a+1}^+ + N_{a+2}^-} \left(T_{a+1} \right)^{N_{a+1}^+} \left(T_{a+2} \right)^{N_{a+2}^-} \hat{J}_{(N_{a+1}^+, N_{a+2}^-)} (-\alpha_{a+1}, +\alpha_{a+2}). \quad (4.6)$$

Recall that factors of T_{a+1}, T_{a+2} originate from aforementioned rescaling of $\tau \rightarrow T\tau$. Taking the saddle-point Eq.(4.4) for T_a 's and α_a 's into Eq.(4.6), convoluting with the external Φ -field insertions, and summing over N_{a+1}^+, N_{a+2}^- , we find factors of the following form:

$$\sum_{N_{a+1}^+, N_{a+2}^-} \left(-\frac{\lambda}{2} \right)^{M_a} \frac{(T_{a+1})^{N_{a+1}^+}}{N_{a+1}^+!} \frac{(T_{a+2})^{N_{a+2}^-}}{N_{a+2}^-!} \int \prod_{i=1}^{M_a} \frac{d^d p_i}{(2\pi)^d} (2\pi)^d \delta(p_1 + \cdots + p_{M_a} - k_a)$$

$$\begin{aligned}
& \times \left[\hat{J}_{(N_{a+1}^+, N_{a+2}^-)} \left(-\alpha_{a+1}, +\alpha_{a+2} \right) \cdot \tilde{\Phi}(p_1) \cdots \tilde{\Phi}(p_{M_a}) \right] \\
= & \sum_{N_{a+1}^+, N_{a+2}^-} \frac{\left(-g|\alpha_{a+1}| \right)^{N_{a+1}^+}}{N_{a+1}^+!} \frac{\left(-g|\alpha_{a+2}| \right)^{N_{a+2}^-}}{N_{a+2}^-!} \int \prod_{i=1}^{M_a} \frac{d^d p_i}{(2\pi)^d} (2\pi)^d \delta(p_1 + \cdots + p_{M_a} - k_a) \\
& \times \left[\hat{J}_{(N_{a+1}^+, N_{a+2}^-)} \left(-\alpha_{a+1}, +\alpha_{a+2} \right) \cdot \tilde{\Phi}(p_1) \cdots \tilde{\Phi}(p_{M_a}) \right] \\
:= & \widehat{W}_{(-\alpha_{a+1}, +\alpha_{a+2})}[\Phi]. \tag{4.7}
\end{aligned}$$

At this stage, \widehat{W} is merely a definition of weighted resummation of the two-loop \star_N -product kernel. Compared to the one-loop \star_N -product kernel, Eq.(4.7) indicates seemingly considerable differences. In particular, Eq.(4.7) depends on two distinct vectors, $\alpha_{a+1}, \alpha_{a+2}$, and involves two exponentiations. Despite the differences, we will shortly show that \widehat{W} is in fact a single open Wilson line, but with a snapped contour!

4.3 Interaction via Snapping of Open Wilson Lines

How precisely is the product \widehat{W} in Eq.(4.7) related to the scalar open Wilson line Eq.(1.3)? Recall that, from the definition Eq.(1.3), shape of the open Wilson line contour was independent of the overall energy-momentum, $\sum_{i=1}^N p_i = k$ or $\theta \cdot \sum_{i=1}^N p_i = \ell$, but depends only on how the the energy-momentum is distributed along the contour. For a *straight* open Wilson line, Eq.(2.3), the energy-momentum was uniformly distributed:

$$W_k[\Phi] = \int d^d x \mathcal{P}_\tau \exp_\star \left(-g|\ell| \int_0^1 d\tau \Phi(x + \ell\tau) \right) \star e^{ik \cdot x}.$$

Taylor-expansion in powers of $(g\ell\Phi)$ yields:

$$\begin{aligned}
W_k[\Phi] = \int d^d x \Big[& e^{ik \cdot x} \\
& + (-g|\ell|) \int_0^1 d\tau \Phi(x + \ell\tau) \star e^{ik \cdot x} \\
& + (-g|\ell|)^2 \int_0^1 d\tau_1 \int_{\tau_1}^1 d\tau_2 \Phi(x + \ell\tau_1) \star \Phi(x + \ell\tau_2) \star e^{ik \cdot x} \\
& + \cdots \Big].
\end{aligned}$$

Fourier-transform Φ 's:

$$\Phi(x + \ell t) = \int \frac{d^d p}{(2\pi)^d} \tilde{\Phi}(p) \mathbf{T}_p \quad \text{where} \quad \mathbf{T}_p := e^{ip \cdot x},$$

where \mathbf{T}_p 's refer to elements of the ‘magnetic translation group’ on the noncommutative space, obeying the \star -product:

$$\mathbf{T}_p \star \mathbf{T}_q = e^{\frac{i}{2}p \wedge q} \mathbf{T}_{p+q},$$

and then evaluate the parametric τ_1, τ_2, \dots integrals. The result is precisely the kernel J_N Eq.(2.1), in terms of which the *scalar* open Wilson lines, Eq.(2.3) were defined. In fact, after Fourier-transforming back to the configuration space, one finds

$$W_k[\Phi] = \sum_{N=0}^{\infty} \int d^d x e^{ik \cdot x} \sum_{N=0}^{\infty} (-g\ell)^N \frac{1}{N!} [\Phi(x) \cdots \Phi(x)]_{\star_N},$$

where the products involved, \star_2, \star_3, \dots , are the \star_N -products. In fact, the \star_N -product is identifiable with the Parisi operator [18]:

$$[\Phi \star_N \Phi]_k := \mathcal{P}_\tau \int d^d x \Phi_1(x, k) \star \Phi_2(x, k) \cdots \Phi_N(x, k) \star \mathbf{T}_k,$$

where

$$\Phi_i(x, k) := \int_0^1 d\tau_i \Phi(x + \ell \tau_i).$$

The result reaffirms that the kernel J_N is Fourier-transform of the \star_N -products.

Compare now the two-loop kernel $\hat{J}_{(N_1^+, N_2^-)}(-\alpha_1, \alpha_2)$ in Eq.(3.17), or, equivalently, the resummed expression $\widehat{W}_{(-\alpha_{a+1}, \alpha_{a+2})}[\Phi]$ in Eq.(4.7) with the open Wilson line definition, Eq.(1.3). Built upon the above discussions, one is led to suspect that \hat{J} arises in the Taylor-series expansion of a version of the open Wilson line, whose contour is along the vectors, $-\alpha_{a+1}$ and α_{a+2} . First, the energy-momentum conservation across a -th boundary holds $\theta \cdot (P_{a+1}^+ + P_{a+2}^-) = \ell_a = (\alpha_{a+2} - \alpha_{a+1})$. Second, the two vectors $\alpha_{a+1}, \alpha_{a+2}$ are not necessarily parallel, so that the contour is snapped into a wedge-shape out of the straight contour ℓ_a . Third, the phase-factor Eq.(3.12) contains the Moyal phase among the momenta within each segment as well as those coming across the two segments. Fourth, the τ -dependent exponential Eq.(3.13) has the same structure as the straight open Wilson line. These observations assert that $\hat{J}_{(N_{a+1}^+, N_{a+2}^-)}(-\alpha_{a+1}, \alpha_{a+2})$ together with the powers of $|\alpha|/2m$ in fact sum up to produce the snapped open Wilson line, which is now identified with $\widehat{W}_{(-\alpha_{a+1}, \alpha_{a+2})}[\Phi]$ in Eq.(4.7)!

Care should be exercised in verifying this conclusion by an explicit computation. Recall that, for one-loop \star_N -product kernel, the moduli parameters are periodic, $\tau_i \rightarrow \tau_i + 1$, reflecting compactness of the one-loop vacuum Feynman diagram. Actually, as quoted in footnote 2, owing to the overall energy-momentum conservation, the kernel J_N for a straight Wilson line is invariant under an arbitrary translation of the moduli: $\tau_i \rightarrow$

$\tau_i + (\text{constant})$. This also implied that, despite its spacetime appearance as an open line, a straight open Wilson line treats all its marked points equally. For a curved open Wilson line, the translation symmetry of moduli parameters is lost, and there ought to be a physically preferred choice of the origin. In view of the geometry of the interaction vertex in Fig. 5, for the snapped open Wilson lines, it is natural to choose the point P as the origin.

5 Final Result

Putting all together, the nonplanar part of the two-loop effective action is expressible as

$$\begin{aligned} \Gamma[W[\Phi]] &= \frac{1}{24} \lambda^2 \hbar^2 \int \frac{d^d k_1}{(2\pi)^d} \cdots \frac{d^d k_3}{(2\pi)^d} (2\pi)^d \delta^{(d)}(k_1 + k_2 + k_3) \\ &\times (4\pi)^{-d} \Delta^{(d-3)/2}(\text{T}) \left(\frac{\Delta(\text{T})}{\Delta_F} \right)^{3/2} \exp\left(-m(|\alpha_1| + |\alpha_2| + |\alpha_3|)\right) \\ &\times \exp\left(-\frac{i}{2} k_1 \wedge k_2\right) \widehat{W}_{(-\alpha_1, \alpha_2)} \widehat{W}_{(-\alpha_2, \alpha_3)} \widehat{W}_{(-\alpha_3, \alpha_1)}. \end{aligned} \quad (5.1)$$

The overall coupling parameters originate from the combinatorics of the two-loop *vacuum* Feynman diagram. The second line is from the saddle-point value of the moduli space integrals, where $\Delta(\text{T})$ and Δ_F are computed and interpreted geometrically in Appendix B and C. In the third line, the phase-factor descends from the factorization, viz. the exponential in Eq.(3.8), while the rest is from resummation of the background Φ -field insertions. Finally, open Wilson lines are summed over the dipole sizes ℓ_a 's, or, equivalently, over the boundary momenta k_a 's, subject to the overall energy-momentum conservation.

Using the defining relation Eq.(3.16), the phase-factor in Eq.(5.1) is expressible as:

$$\exp\left(-\frac{i}{2} k_1 \wedge k_2\right) = \exp\left(\frac{i}{2} \alpha_1 \mathbf{V} \alpha_2\right) \exp\left(\frac{i}{2} \alpha_2 \mathbf{V} \alpha_3\right) \exp\left(\frac{i}{2} \alpha_3 \mathbf{V} \alpha_1\right),$$

where \mathbf{V} is a shorthand notation for wedge product with respect to $(\theta^{-1})_{mn}$. Redefining the snapped open Wilson line so that each exponential is absorbed into it:

$$\exp\left(\frac{i}{2} \alpha_1 \mathbf{V} \alpha_2\right) \widehat{W}_{(-\alpha_1, \alpha_2)}[\Phi] \longrightarrow \widehat{W}_{(-\alpha_1, \alpha_2)}[\Phi],$$

the open Wilson lines in Eq.(5.1) are interpretable as matrices, whose row and column are indexed by $\{\alpha_a\}$, and their product corresponds to matrix multiplication!⁸ Thus, while the open Wilson lines are naturally interpreted as composite operators describing a

⁸ Note that the phase-factor absorbed vanishes identically for *straight* open Wilson lines, and hence does not modify functional form of the result, Eq.(1.2).

‘closed string’, they seem to obey a noncommutative and associative algebra, rather than a commutative and non-associative one.

Finally, introduce shorthand notations

$$\begin{aligned} \left(-\frac{\lambda}{2}\right)^2 &:= \lambda_c \\ \int \prod_{a=1}^3 \frac{d^d k_a}{(2\pi)^d} (2\pi)^d \delta(k_1 + k_2 + k_3) &:= \text{Tr}_{\mathcal{H}_{\text{dipole}}} \\ (4\pi)^{-d} \Delta(T)^{(d-3)/2} \left(\frac{\Delta(T)}{\Delta_F}\right)^{3/2} \prod_{a=1}^3 \exp(-m|\alpha_a|) &:= \mathbf{K}_3(\{\alpha_a\}), \end{aligned}$$

the first being strongly reminiscent of the ‘soft-dilaton theorem’ [19] in string theory. Then, Eq.(5.1) is re-expressible compactly as:

$$\Gamma_2[W] = \frac{\lambda_c}{3!} \text{Tr}_{\mathcal{H}_{\text{dipole}}} \mathbf{K}_3(\{\alpha_a\}) \left(\widehat{W} \star \widehat{W} \star \widehat{W} \right),$$

obtaining the proclaimed main result, Eq.(1.4). The \star ’s are to emphasize that the product involved are matrix multiplication, viz. the newly emergent noncommutative geometry obeyed by the open Wilson lines.

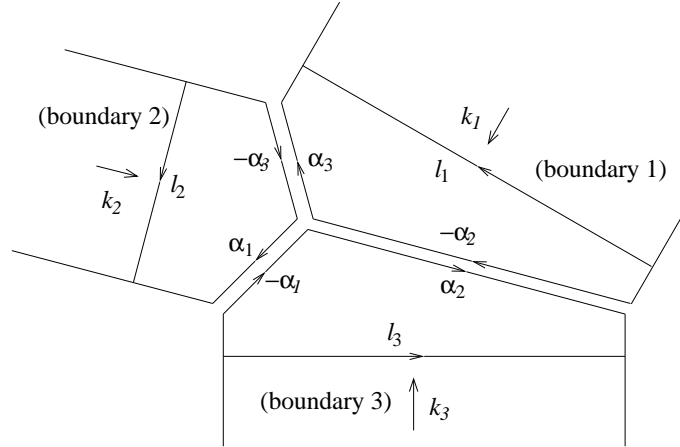


Figure 7: *Spacetime view of the cubic interaction among the noncommutative dipoles created by the open Wilson line operators.*

Pictorially, the cubic interaction among the ‘closed string’ states created by the open Wilson line operators is depicted in Fig.7. The interaction goes as follows. At asymptotic infinity, three *straight* noncommutative dipoles, viz. free ‘closed strings’, approach one another. Near the interaction point P , each dipole snaps its contour dynamically so that the interaction with adjacent dipoles is purely local and maximally overlapping.

Note that the effective action, once expressed in terms of the snapped open Wilson lines, is remarkably similar to the half-string formulaton [20, 21] of Witten’s open string

field theory [22], though the noncommutative dipoles are interpretable most naturally as ‘closed strings’. A minor difference is that location of P is determined *dynamically* by the energy-momenta of the asymptotic dipoles, while, in Witten’s open string field theory, it is fixed at the midpoint once and for all, breaking the worldsheet reparametrization invariance. We trust that the similarity is far more than a mere coincidence, and further elaboration of the relation will be reported elsewhere.

Finally, in light of the ubiquity of the open Wilson lines, precisely the same result and physical interpretation can be drawn for noncommutative field theories, including noncommutative gauge theories⁹ and those with supersymmetries. Explicit verification for such theories are straightforward, and will be reported in forthcoming papers.

Acknowledgements

We acknowledge enlightening discussions with Costas Bachas, Hong Liu, Peter Mayr, Jeremy Michelson, Ashoke Sen, Erik Verlinde, Herman Verlinde, and Jung-Tay Yee. SJR thanks warm hospitality of CERN Theory Division, Spinoza Institute at Utrecht University, Summer Institute 2001 at Yamanashi-Japan, and Ecole de Physique Les Houches, where substantial parts of the present work were accomplished.

Appendix

A Two-Loop Feynman Diagrammatics

In this appendix, we will elaborate derivation of Eqs.(3.1, 3.2) via the noncommutative Feynman diagrammatics. The noncommutative Feynman rules of $\lambda[\Phi^3]_\star$ -theory are summarized, in the background field method, by the following generating functional:

$$Z[\Phi_0] = Z_0[\Phi_0] \int \mathcal{D}\varphi \exp \left(- \int d^d x \left[\frac{1}{2} \varphi(x) (-\partial_x^2 + m^2 + \lambda \Phi_0(x)) \varphi(x) + \frac{\lambda}{3!} \varphi^3(x) \right] \right) \quad (\text{A.1})$$

Here, $\Phi_0(x)$ and $\varphi(x)$ refer to the background and the fluctuation parts of the scalar field, Φ , respectively. In the notations and conventions explained in the previous subsection, the two-loop Feynman integral of the N-point, one-particle-irreducible Green function is given, after Wick rotation to the Euclidean space, by

$$\Gamma_N = (-\lambda)^{N+2} C_{\{N\}} \int \frac{dq_1}{(2\pi)^d} \frac{dq_2}{(2\pi)^d} \prod_{a=1}^3 \left(\prod_{i=0}^{N_a} \frac{1}{(q_a + \sum_{j=1}^i p_j^{(a)})^2 + m^2} \right) \quad (\text{A.2})$$

⁹A step toward this direction is made in [24].

$$\times \exp \left[\frac{i}{2} (q_1 \wedge q_2 - (q_1 + P_1) \wedge (q_2 + P_2)) \right] \exp \left[-\frac{i}{2} \sum_{i=1}^{N_a} \left(q_a + \sum_{j=1}^{i-1} p_j^{(a)} \right) \wedge p_i^{(a)} \nu_i^{(a)} \right].$$

Here, q_a 's denote the momentum flowing through the a -th internal propagator ($a = 1, 2, 3$), and are subject to the momentum conservation, $q_1 + q_2 + q_3 = 0$. As compared to the commutative counterpart, the integrand in Eq.(A.2) is modified by the two phase-factors arising from the Moyal's product in Eq.(A.1). The first phase-factor originates from Moyal's product present in the two cubic interaction vertices. The second originates from insertion of each external line, and depends on ν ¹⁰.

To facilitate the integration, introduce the Feynman-Schwinger parametric representation to each of the total $(N+3)$ propagators:

$$\left[\frac{1}{\left(q_a + \sum_{j=1}^i p_j^{(a)} \right)^2 + m^2} \right] = \int_0^\infty ds_i^{(a)} \exp \left[-s_i^{(a)} \left(\left(q_a + \sum_{j=1}^i p_j^{(a)} \right)^2 + m^2 \right) \right].$$

Decompose $s_i^{(a)}$'s into N 'insertion position moduli' parameters τ_i 's and the 'vacuum moduli' T_a 's:

$$\begin{aligned} T_a &:= \sum_{j=0}^{N_a} s_j^{(a)} = \tau_0^{(a)} & (a = 1, 2, 3) \\ \tau_i^{(a)} &:= \sum_{j=i}^{N_a} s_j^{(a)} & (i = 1, 2, \dots, N_a). \end{aligned} \quad (\text{A.3})$$

The Jacobian in changing variables from $(s_0^{(a)}, \dots, s_{N_a}^{(a)})$ to $(T_a, \tau_1^{(a)}, \dots, \tau_{N_a}^{(a)})$ is evidently unity. In terms of the newly introduced moduli parameters, Eq.(A.3), the string of propagators along each of the three vacuum internal lines is expressible as:

$$\begin{aligned} \prod_{a=1}^3 \prod_{i=0}^{N_a} \left(\frac{1}{\left(q_a + \sum_{j=1}^i p_j^{(a)} \right)^2 + m^2} \right) &= \prod_{a=1}^3 \int_0^\infty dT_a \int d\tau_1^{(a)} \dots d\tau_{N_a}^{(a)} e^{-m^2 T_a} \\ &\times \exp \left[-T_a (q_a)^2 - 2q_a \cdot \sum_{i=1}^{N_a} p_i^{(a)} \tau_i^{(a)} - \sum_{i=1}^{N_a} p_i^{(a)} \cdot p_i^{(a)} \tau_i^{(a)} - 2 \sum_{i < j}^{N_a} p_i^{(a)} \cdot p_j^{(a)} \tau_j^{(a)} \right]. \end{aligned} \quad (\text{A.4})$$

Here, the $\tau^{(a)}$ -integrations are defined over $0 \leq \tau_{N_a}^{(a)} \leq \dots \leq \tau_1^{(a)} \leq T_a \leq \infty$. One can readily show that, once summed over all possible permutations of external insertions along each vacuum internal line, all the $\tau_i^{(a)}$ -integrations are extended over $[0, T_a)$.

¹⁰The convention we adopt for the Feynman rules is that all phase-factors reside at the interaction vertices. In the convention adopted in the worldline formulation [15], an overall phase is assigned for each diagram and, at the same time, for nonplanar an appropriate extra phase-factor is attached for each nonplanar crossing. It can be shown straightforwardly that the two phase-factor conventions produce identical results.

Next, we evaluate the integrals over the loop momenta $q^{(1)}$ and $q^{(2)}$. Recall first how the integrals are evaluated in the commutative case, where the two exponential functions in Eq.(A.2) involving noncommutative phase-factors are absent. Collecting the $q^{(a)}$ -dependent part in the exponent of Eq.(A.4):

$$-T_1(q_1)^2 - T_2(q_2)^2 - T_3(q_1 + q_2)^2 - 2q_1 \cdot A_1 - 2q_2 \cdot A_2 + 2(q_1 + q_2) \cdot A_3, \quad (\text{A.5})$$

where $A_a := (\sum p_i \tau_i)_a$, and expressing the quadratic polynomial into a complete-square function, the integrals over q_1, q_2 can be performed successively as Gaussian integrals. One can express the result ¹¹ compactly as ¹²:

$$\Delta^{\frac{d}{2}}(T) \left(\prod_{a=1}^3 e^{-m^2 T_a} \right) \exp \left[\frac{1}{2} \sum_{i=1}^{N_a} \sum_{j=1}^{N_b} G_{ab}^{(0)} \left(\tau_i^{(a)}, \tau_j^{(b)} \right) p_i^{(a)} \cdot p_j^{(b)} \right], \quad (\text{A.6})$$

where

$$\begin{aligned} G_{aa}^{(0)}(x, y) &= |x - y| - \Delta (T_{a+1} + T_{a+2}) (x - y)^2, \\ G_{aa+1}^{(0)}(x, y) &= x + y - \Delta \left(x^2 T_{a+1} + y^2 T_a + (x - y)^2 T_{a+2} \right), \end{aligned}$$

and account for, in Eq.(3.2), the T_a -dependent weight functions in the first line, and the first exponential in the second line.

We now turn to the phase-factors arising from the noncommutative Feynman rules. They arise from the two cubic interaction vertices, viz. the phase-factor of the first exponential in Eq.(A.2):

$$\frac{i}{2} q_1 \wedge q_2 - \frac{i}{2} (q_1 + P_1) \wedge (q_2 + P_2) = -\frac{i}{2} q_1 \wedge P_2 + \frac{i}{2} q_2 \wedge P_1 - \frac{i}{2} P_1 \wedge P_2, \quad (\text{A.7})$$

and from the external insertions, viz. the phase-factor in the second exponential in Eq.(A.2):

$$-\frac{i}{2} \sum_{i=1}^N \left(q_a + \sum_{j=1}^{i-1} p_j^{(a)} \right) \wedge p_i^{(a)} \nu_i^{(a)} \quad (\text{A.8})$$

¹¹ The result is identical to those presented in [16], where the relationship between the worldline propagators, G_{ab} , and the string theory worldsheet propagators are elaborated in detail.

¹² In obtaining the result, the following identities resulting from momentum conservation have been used:

$$\begin{aligned} - \left[\sum_i p_i^2 \tau_i + 2 \sum_{i < j} p_i \cdot p_j \tau_j \right]_a &= \left[\sum_{i < j} p_i \cdot p_j \tau_{ij} \right]_a + A_a (P_{a+1} + P_{a+2}) \\ - \left[\sum_i p_i^2 \tau_i^2 + 2 \sum_{i < j} p_i \cdot p_j \tau_i \tau_j \right]_a &= \left[\sum_{i < j} p_i \cdot p_j \tau_{ij}^2 \right]_a + \left(\sum p_i \tau_i^2 \right)_a (P_{a+1} + P_{a+2}). \end{aligned}$$

$$= -\frac{i}{2}q_a \wedge (P_a^+ - P_a^-) - \frac{i}{2}P_a^- \wedge P_a^+ - \frac{i}{4} \sum_{i < j}^{N_a} p_i^{(a)} \wedge p_j^{(a)} (\nu_i^{(a)} + \nu_j^{(a)}) \epsilon(\tau_{ij}^{(a)})$$

along each a -th internal line. First, note that the moduli-independent phase-factors from Eqs.(A.7,A.8) combine and yield the exponential with moduli-independent phase-factors (via momentum conservation $P_1 + P_2 + P_3 = 0$)

$$\exp \left[-\frac{i}{2} \sum_{a=1}^3 (P_a^- \wedge P_a^+) - \frac{i}{2} P_1 \wedge P_2 \right] = \exp \left[-\frac{i}{2} \sum_{a=1}^3 \left(P_a^- \wedge P_a^+ + \frac{1}{3} P_a \wedge P_{a+1} \right) \right], \quad (\text{A.9})$$

and an exponential with $\epsilon(\tau_{ij}^{(a)})$ -dependent phase-factors

$$\exp \left[-\frac{i}{4} \sum_{i < j}^{N_a} p_i^{(a)} \wedge p_j^{(a)} (\nu_i^{(a)} + \nu_j^{(a)}) \epsilon(\tau_{ij}^{(a)}) \right]. \quad (\text{A.10})$$

They account for the two exponentials in Eq.(3.2): Ξ_1, Ξ_2 , respectively.

Note that, in Eq.(A.7), terms quadratic in $q^{(a)}$ cancel each other. This is inherited to the fact that, as mentioned in footnote 3, the two-loop vacuum diagram under consideration descends, in the Seiberg-Witten limit of bosonic string theory, from disk worldsheet with two holes or, equivalently, from sphere worldsheet with three holes, and hence referred it as *planar* vacuum diagram. If one of the propagators emanating from the first interaction vertex were twisted before joining the second vertex, the resulting vacuum diagram is *nonplanar*, for which the sign of the second term in the first expression of Eq.(A.7) is reversed. Thus, for nonplanar diagrams, terms quadratic in $q^{(a)}$'s, $i q^{(1)} \wedge q^{(2)}$, are produced¹³.

Cancellation of terms quadratic in $q^{(a)}$'s puts the rest of the computation straightforward. Collect terms linear in q_a :

$$-\frac{i}{2} [q_1 \wedge (P_1^+ - P_1^-) + q_2 \wedge (P_2^+ - P_2^-) - (q_1 + q_2) \wedge (P_3^+ - P_3^-) + q_1 \wedge P_2 - q_2 \wedge P_1] \quad (\text{A.11})$$

add this to Eq.(A.5), and perform the integrations over q_1 and q_2 . As the quadratic parts in the exponent are not modified, compared to the commutative case Eq.(A.6), the integration results in two extra phase-factors: a \wedge -product originating from cross terms between Eq.(A.5) and Eq.(A.11), and a \circ -product originating from the square of Eq.(A.11). The two extra phase-factors are further simplifiable in terms of the *worldsheet boundary* momenta k_a :

$$\exp \Delta \sum_{a=1}^3 \left(i T_a k_a \wedge (A_{a+2} - A_{a+1}) - \frac{1}{4} T_a k_a \circ k_a \right).$$

¹³In [15], it was shown that the nonplanar diagram contribution to the N-point Green function can be related to the planar diagram contribution via insertion of a pseudo-differential operator, $\exp(-i\partial_z \wedge \partial_w)|_{z=w=x_2}$, where x_2 refers to the spacetime position of the second interaction vertex.

This accounts for, in Eq.(3.2), the second exponential in the second line and the last phase-factor, Ξ_3 .

B Saddle-Point Analysis

The saddle point condition should determine the saddle point value of T_a 's in terms of l_a 's. In this Appendix, we sketch a method to achieve that task and determine L as a consequence.

The saddle point condition demands that the three vectors $(\alpha_a/t_a) = t_{a+1}l_{a+1} - t_{a+2}l_{a+2}$ form an equilateral triangle. The length of the vectors is defined to be L . The products of $l_a = \alpha_{a+2} - \alpha_{a+1}$ thus take the simple form:

$$2l_a \cdot l_{a+1} = (1 - 2t_{a+2}(t_1 + t_2 + t_3))L^2, \quad (\text{B.1})$$

$$l_a^2 = (t_{a+1}^2 + t_{a+2}^2 + t_{a+1}t_{a+2})L^2, \quad (\text{B.2})$$

We have used the normalization condition $(t_1t_2 + t_2t_3 + t_3t_1 = 1)$ to simplify Eq.(B.1). One way to solve these equations is as follows. First, we rewrite Eq.(B.1) as

$$t_{a+2} = \frac{L^2 - 2l_a \cdot l_{a+1}}{2L^2(t_1 + t_2 + t_3)}. \quad (\text{B.3})$$

We then sum up Eq.(B.2), and find

$$2L^2(t_1 + t_2 + t_3)^2 = l_1^2 + l_2^2 + l_3^2 + 3L^2. \quad (\text{B.4})$$

We can use Eq.(B.4) to eliminate $(t_1 + t_2 + t_3)$ from Eq.(B.3),

$$t_{a+2} = \frac{L^2 - 2l_a \cdot l_{a+1}}{\sqrt{2L^2(l_1^2 + l_2^2 + l_3^2 + 3L^2)}}. \quad (\text{B.5})$$

Plugging the $\{t_a\}$ of Eq.(B.5) into the normalization condition and further using momentum conservation determines L :

$$\begin{aligned} 3L^4 &= 4\{(l_1 \cdot l_2)(l_2 \cdot l_3) + (l_2 \cdot l_3)(l_3 \cdot l_1) + (l_3 \cdot l_1)(l_1 \cdot l_2)\} \\ &= -(l_1^4 + l_2^4 + l_3^4) + 2(l_1^2l_2^2 + l_2^2l_3^2 + l_3^2l_1^2). \end{aligned}$$

Comparing the last line with Heron's formula [23] for the area of a triangle, we find that

$$\frac{\sqrt{3}}{4}L^2 = \text{Area}(l_1, l_2, l_3). \quad (\text{B.6})$$

Note that the left-hand-side is the area of the *equilateral* triangle whose sides have the length L , while the right-hand-side is the area of the triangle formed out of $\{l_a\}$. The

expressions Eq.(B.5) and Eq.(B.6) explicitly determine the saddle point t_a (and thus T_a) in terms of l_a 's, from which we can compute every quantities of interests at the saddle point.

If we are interested in deriving Eq.(B.6) only, there is a simpler way, though it does not give the value of t_a . Recall that $\{\alpha_a\}$ divide the triangle into three disjoint pieces. The area of the triangle is then given by

$$\begin{aligned} A &= \frac{1}{2}|\alpha_1||\alpha_2|\sin(2\pi/3) + \frac{1}{2}|\alpha_2||\alpha_3|\sin(2\pi/3) + \frac{1}{2}|\alpha_3||\alpha_1|\sin(2\pi/3) \quad (\text{B.7}) \\ &= \frac{\sqrt{3}}{4}L^2(t_1t_2 + t_2t_3 + t_3t_1) = \frac{\sqrt{3}}{4}L^2, \end{aligned}$$

where we have used the normailzation condition, obtaining the final result.

C Computation of $(\Delta_F)^{-3/2}$

Recall that the form of the exponent is given by

$$F = -m^2(T_1 + T_2 + T_3) - \frac{1}{4}\Delta(T)(T_1l_1^2 + T_2l_2^2 + T_3l_3^2) .$$

The saddle point conditions are

$$\frac{\partial F}{\partial T_a} = -m^2 + \frac{\Delta^2}{4}(T_{a+1}l_{a+1} - T_{a+2}l_{a+2})^2 = 0 .$$

The second derivatives of F at the saddle point turn out to be

$$\begin{aligned} \frac{\partial^2 F}{\partial T_a^2} &= -4(t_{a+1} + t_{a+2})\frac{m^3}{L} , \\ \frac{\partial^2 F}{\partial T_a \partial T_{a+1}} &= -2t_{a+2}\frac{m^3}{L} . \end{aligned}$$

The width of the saddle is thus given by

$$\begin{aligned} (\Delta_F)^{-3/2} &= (2\pi)^{3/2} \det \left(\frac{\partial^2 F}{\partial T_a \partial T_b} \right)^{-1/2} \\ &= \left(\frac{\pi^3 L^3}{6m^9} \right)^{1/2} (t_1 + t_2 + t_3)^{-1/2} . \end{aligned}$$

It is worth noting that the dimensionless width is expressible as

$$\left(\frac{32\pi^3}{3} \right)^{-1/2} \left(\frac{\Delta(T)}{\Delta_F} \right)^{3/2} = (mL)^{-3/2} (t_1 + t_2 + t_3)^{-1/2} = (m^3 L^2 (|\alpha_1| + |\alpha_2| + |\alpha_3|))^{-1/2} .$$

References

- [1] S. Minwalla, M. Van Raamsdonk and N. Seiberg, JHEP **0002**, 020 (2000) [arXiv:hep-th/9912072].
- [2] S.-J. Rey and R. von Unge, Phys. Lett. **B499**, 215 (2001) [arXiv:hep-th/0007089].
- [3] S. R. Das and S.-J. Rey, Nucl. Phys. **B 590**, 453 (2000) [arXiv:hep-th/0008042].
- [4] N. Ishibashi, S. Iso, H. Kawai and Y. Kitazawa, Nucl. Phys. **B 573**, 573 (2000) [arXiv:hep-th/9910004];
J. Ambjorn, Y. M. Makeenko, J. Nishimura and R. J. Szabo, JHEP **0005**, 023 (2000) [arXiv:hep-th/0004147];
D.J. Gross, A. Hashimoto and N. Itzhaki, [arXiv:hep-th/0008075];
Y. Okawa and H. Ooguri, Nucl. Phys. B **599**, 55 (2001) [arXiv:hep-th/0012218].
- [5] S.-J. Rey, *Exact Answers to Approximate Questions: Noncommutative Dipole, Open Wilson Line, and UV-IR Duality*, Proceedings of ‘New Ideas in String Theory’, APCTP-KIAS Workshop (June, 2001) and of ‘Gravity, Gauge Theories, and Strings’, Les Houches Summer School (August, 2001), to appear.
- [6] N. Read, Semicond. Sci. Technol. **9** (1994) 1859; Surf. Sci. **361** (1996) 7; V. Pasquier, (unpublished); R. Shankar and G. Murthy, Phys. Rev. Lett. **79** (1997) 4437; D.-H. Lee, Phys. Rev. Lett. **80** (1998) 4745; V. Pasquier and F.D.M. Haldane, Nucl. Phys. **B 516**[FS] (1998) 719; A. Stern, B.I. Halperin, F. von Oppen and S. Simon, Phys. Rev. **B 59** (1999) 12547.
- [7] D. Bigatti and L. Susskind, Phys. Rev. **D 62**, 066004 (2000) [arXiv:hep-th/9908056];
Z. Yin, Phys. Lett. **B 466**, 234 (1999) [arXiv:hep-th/9908152];
H. Liu and J. Michelson, Phys. Rev. **D 62**, 066003 (2000) [arXiv:hep-th/0004013].
- [8] Y. Kiem, S. Lee and D.-H. Park, Phys. Rev. **D 63**, 126006 (2001), [arXiv:hep-th/0011233].
- [9] Y. Kiem, S.-J. Rey, H.-T. Sato and J.-T. Yee, *Open Wilson lines and generalized star product in noncommutative scalar field theories*, to appear in Phys. Rev. **D** (2001) [arXiv:hep-th/0106121].
- [10] Y. Kiem, S.-J. Rey, H.-T. Sato and J.-T. Yee, *Anatomy of one-loop effective action in noncommutative scalar field theories*, [arXiv:hep-th/0107106].

- [11] S. R. Das and S.-J. Rey, Phys. Lett. B **186**, 328 (1987);
J. Khoury and H. Verlinde, Adv. Theor. Math. Phys. **3**, 1893 (1999) [arXiv:hep-th/0001056].
- [12] M. R. Garousi, Nucl. Phys. B **579**, 209 (2000) [arXiv:hep-th/9909214].
- [13] H. Liu, [arXiv:hep-th/0011125].
- [14] T. Mehen and M. B. Wise, JHEP **0012**, 008 (2000) [arXiv:hep-th/0010204].
- [15] Y. Kiem, S.-S. Kim, S.-J. Rey and H.-T. Sato, *Anatomy of Two-Loop Effective Action in Noncommutative Field Theories*, [arXiv:hep-th/0110066].
- [16] K. Roland and H.-T. Sato, Nucl. Phys. B **515** (1998) 488; *ibid*, Nucl. Phys. B **480** (1996) 99.
- [17] Y. Kiem, S. Lee and J. Park, Nucl. Phys. B **594**, 169 (2001) [arXiv:hep-th/0008002].
- [18] G. Parisi, Phys. Lett. B **112**, 463 (1982).
- [19] M. Ademollo, A. D’Adda, R. D’Auria, F. Gliozzi, E. Napolitano, S. Sciuto and P. Di Vecchia, Nucl. Phys. B **94**, 221 (1975);
S.-J. Rey, Phys. Lett. B **203**, 393 (1988); *ibid*, Nucl. Phys. B **316**, 197 (1989);
T. Yoneya, Phys. Lett. B **197**, 76 (1987);
R. C. Myers, S. Penati, M. Pernici and A. Strominger, Nucl. Phys. B **310**, 25 (1988);
A. Belopolsky and B. Zwiebach, Nucl. Phys. B **472**, 109 (1996) [arXiv:hep-th/9511077].
- [20] J. Bordes, H. M. Chan, L. Nellen and S. T. Tsou, Nucl. Phys. B **351**, 441 (1991);
F. Anton, A. Abdurrahman and J. Bordes, Nucl. Phys. B **397**, 260 (1993) [arXiv:hep-th/9305166].
- [21] L. Rastelli, A. Sen and B. Zwiebach, [arXiv:hep-th/0105058];
D. J. Gross and W. Taylor, JHEP **0108**, 009 (2001) [arXiv:hep-th/0105059];
T. Kawano and K. Okuyama, JHEP **0106**, 061 (2001) [arXiv:hep-th/0105129];
D. J. Gross and W. Taylor, JHEP **0108**, 010 (2001) [arXiv:hep-th/0106036].
- [22] E. Witten, Nucl. Phys. B **268**, 253 (1986).
- [23] See, for instance, Y. Id and E.S. Kennedy, Math. Teacher **62**, 585-587 (1969);
C.M. Taisbak, Centaurus **24**, 110-116 (1981); (E) **25**, 160 (1981/1982).
- [24] A. Armoni and E. Lopez, [arXiv:hep-th/0110113].